04

Dynamics of structure of pulsed discharge in nitrogen and argon at different pressures in a „pin to plane“ gap

© A.A. Trenkin, K.I. Almazova, A.N. Belonogov, V.V. Borovkov, A.S. Dolotov, I.V. Morozov

Russian Federal Nuclear Center, All-Russia Research Institute of Experimental Physics,
607190 Sarov, Russia
e-mail: alexey.trenkin@gmail.com

Received March 23, 2022
Revised April 20, 2022
Accepted May 4, 2022

Using high-speed shooting and shadow photography, the spatial structure of a pulsed discharge in a 1.5 mm long „pin(cathode)−plane“ gap in nitrogen and argon in the pressure range from 0.25 to 2 atm was studied. It has been found that a spark discharge is realized in nitrogen and a diffuse form of discharge is realized in argon. For both cases, the presence of a microstructure of discharges in the studied pressure range was found, when the discharge is an aggregation of a large number of micron-diameter channels. It is shown that for each gas the dynamics of the discharge glow structure remains similar at different pressures. It has been established that the glow and microstructure of the discharge in nitrogen are similar to those in air.

Keywords: spark discharge, diffuse discharge, microstructure, method of shadow photography, high-speed shooting.

DOI: 10.21883/TP.2022.09.54678.58-22

Introduction

Understanding the set of processes occurring in gas discharges is important both from a fundamental point of view and in terms of the development of gas discharge technologies. For example, high-voltage pulsed gas discharges are widely used in plasma-chemical reactors [1–3], plasma actuators [4–6], electric-discharge gas lasers [7–9], in surface treatment [10].

Despite a long period of research, a number of gas-discharge phenomena remain poorly understood. They include the discharge microstructure [11–25], when the current channel is a set of a large number of microchannels (filaments). The microstructure was detected during discharges in air at atmospheric pressure: initially by the autograph method on the surface of a flat electrode [11–18], then by shadow and interference methods of high space-time resolution in the volume of the discharge gap [18–25]. Especially note that the microchannel structure against the background of the discharges glow was unresolvable by optical and electron-optical methods [19]. It was established that the microstructure appears in the initial phase of the discharge and exists later, and it seems that the mechanism of its formation is the instability of the ionization wave front (see [24] and references therein). It was also shown that the presence of the microstructure can provide a number of specific effects that are absent in structureless (uniform) channels: generation of high-energy electrons in microchannels, acceleration of channel heads in the phase of gap bridging, increased electron temperatures and other [25−28].

It appears, however, that the presence of the discharges microstructure is deprived of due attention both in terms of this phenomenon accounting in computational-theoretical modeling, and in practical gas-discharge technologies. In particular, this may be due to the idea of this phenomena „specific nature“, i.e. its realization in a narrow range of conditions. At the same time, the microstructure was found in many types of discharges: in diffuse form of discharges in the gap „rod−plane“, „wire parallel to the plane“ [11,14,15,18]; barrier and spark discharges in geometry „pin−plane“ and in homogeneous gaps [12,16–25]; in a streamerless discharge in a homogeneous gap [13]. Note, however, that all of these discharges are realized in air at atmospheric pressure. Therefore, the development of the idea of the degree of the microstructure spreading requires expanding the conditions for the implementation of gas discharges (types of gases and their mixtures, pressure of the working medium, parameters of the supply voltage, electrode configurations) and studying the microstructure presence in them. In this connection, in this paper we studied the spatial structure of discharges in nitrogen and argon in the pressure range of 0.25 to 2 atm.

1. Experimental equipment and methods

The diagram of the experimental bench is presented in Fig. 1. A part of its elements are characterized in detail in [19,21]. Pulsed voltage generator ensured negative polarity output pulse with an amplitude of 25 kV and a level 0.1−0.9 rise time of approximately 7 ns. The pulse was applied to discharge gap through the cable line 7 m long. Voltage and current measurements were performed at the pulsed voltage generator output by means of a capacitance divider and resistive shunt, accordingly. The temporal resolution of the divider and the shunt was no worse

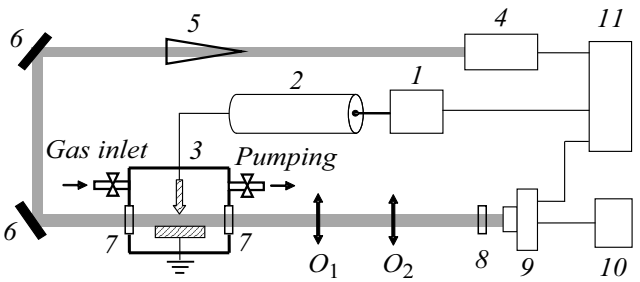

Figure 1. Schematic diagram of the experimental stand: *1* — voltage pulse generator, *2* — cable line, *3* — vacuum chamber with a discharge gap, *4* — probing radiation source (laser), *5* — collimator, *6* — turning mirror, *7* — window, O_1 and O_2 — lenses, *8* — light filters, *9* — electron-optical recorder, *10* — personal computer, *11* — synchronization unit.

than 1 ns. Signals were recorded using an oscilloscope with a bandwidth of 500 MHz and a digitizing rate of 2 Gs/s.

The electrode system had a „pin–plane" geometry. An axially symmetric pin electrode is fabricated from stainless steel and had a length of 19 mm, diameter of 14 mm, an apex angle of 36°, and a curvature radius of 0.15 mm. A plane electrode was fabricated from an aluminum alloy and had the working part close in shape to a segment of a sphere with a diameter of 4.5 cm and a thickness of 1.5 cm. The interelectrode gap was 1.5 mm.

The electrode system was placed coaxially inside a cylindrical metal vacuum chamber. Chamber diameter is 310 mm, height is 800 mm. Input and output of laser radiation was carried out through chamber windows made of KU-1 glass with a diameter of 80 mm and a thickness of 15 mm. The evacuation and gas puffing system provided the working medium for the different gases discharge at different pressures. In this paper, we used: nitrogen in the pressure range of 0.25 to 1 atm and argon — 0.5 to 2 atm.

An optical discharge detection system was used as a part of the stand. The system included a probing radiation source — solid-state laser (wavelength of 532 nm and a pulse duration at 50% of 6 ns), collimator, lenses, light filters, and digital electron-optical camera. A plane-parallel laser beam crossed the discharge region at a right angle to the spike–electrode axis and was detected by the electron-optical camera. The laser beam at the discharge generation region had a crosswise size of approximately 1 cm and a Gaussian profile. Since the interelectrode gap is far less than the bundle size, it ensured a homogeneous enough field of the laser radiation within the discharge region.

The vacuum chamber use, in contrast to previous experiments [19–21,24], required the optical scheme change. Additional lens O_1 was used, which was located at a double focal length from the discharge gap and made its image in a scale of 1 : 1. Then lens O_2 transferred this image with zoom 10 : 1 to the photocathode of the electron-optical recorder.

Shadow photography methodology is based on the described stand. The exposure of each frame was set by the laser pulse duration. The frames were timed relative to the moment of breakdown, and the time characterizing them corresponds to the start of imaging.

The laser was not used in the experiments on shooting the glow of the discharge. The frame exposure of the electron-optical recorder was 40 ns. When shooting the early stages of the discharge (at times below 40 ns), part of the exposure time was ahead of the beginning of the discharge formation. The linking of the frame of the glow discharge was determined by the moment of the shutter closing of the electron-optical recorder.

The registration system worked in single-frame mode i.e. one frame per pulse. Different stages of the discharge process were visualized by shifting the moments of actuation of the laser and the electron-optical detector relative to the moment of breakdown. The resolving power of the optical system was 5 μm per three pixels.

2. Experimental results and discussion

Based on the results of earlier studies [19–21,24] of a discharge in air at atmospheric pressure, we note its main characteristics. An oscillatory process with exponential current and voltage decay was initiated in the discharge circuit after the breakdown of the gap. The oscillation period was 0.6 μs, and the amplitude and the decay time of current were 1 kA and 1.2 μs, respectively. At the same time, two characteristic moments were distinguished on oscillograms: occurrence of voltage within the discharge gap t_U and breakdown. The onset of the current rise (and the voltage decay) was assumed to be the moment of breakdown t_{br}.

In previous papers [19–21,24] the following dynamics of the spatial structure of the initial phase of the discharge in air was registered. In the pre-breakdown stage a weakly luminous diffuse channel and cathode spots appear, then in the interval from 5 to 15 ns, luminous formations propagate from the cathode, and the gap is closed by a uniform, brightly luminous channel. The shadow patterns show that the channel is set of microchannels, which are unresolvable in the discharge glow photographs. The microstructure is registered on the shadow patterns from the first nanoseconds after the breakdown.

Fig. 2 shows the initial fragments of voltage U and current I oscillograms at various pressures in nitrogen. In the time interval from 0 to 60 ns, electrical signals propagate along the cable line. The rise of voltage and current decreasing in the interval between t_U and t_{br} corresponds to the voltage wave reflection from the initially open end of the cable line. It can be seen that the oscillograms of the initial phase of the discharge at different pressures do not contain significant differences. A similar situation was also observed for oscillograms during discharge in argon.

Fig. 3 shows frames of the glow of the discharge in nitrogen at pressure of 1 atm, and Fig. 4 — at pressure of 0.25 atm at different times. In the initial phase cathode spots and weakly luminous diffuse channel appear, then

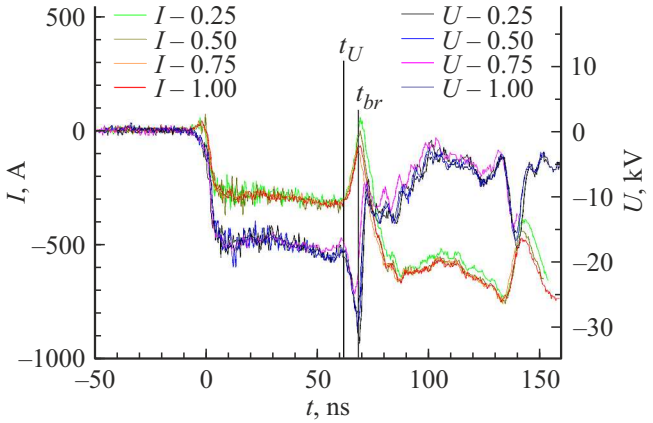

Figure 2. Initial fragments of voltage U and current I oscillograms at different nitrogen pressures (t_U — moment of voltage appearance across the discharge gap; t_{br} — moment of breakdown; pressure is indicated on inserts in atm).

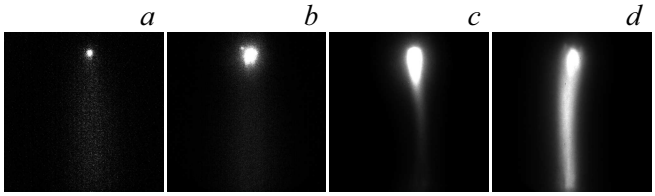

Figure 3. Photographs of the glow of the discharge in nitrogen at pressure of 1 atm at different times: *a* — 1, *b* — 4, *c* — 13, *d* — 23 ns.

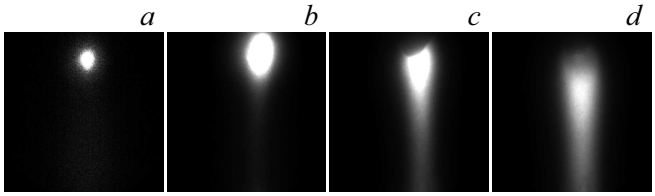

Figure 4. Photos of the glow of discharge in nitrogen at pressure of 0.25 atm at different times: *a* — 5, *b* — 25, *c* — 38, *d* — 60 ns.

luminous formations propagate from the cathode, and the gap is closed by a uniform, brightly luminous channel. Comparison of the data obtained indicates a delay in the evolution of the discharge glow structure relative to the onset of breakdown with pressure decreasing; however, the morphology of the structure retains similarity at different pressures. Comparison of photos of the glow of the discharge in nitrogen and air [18,20] at atmospheric pressure shows the similarity of the dynamics of the glow structure in these gases.

Fig. 5 shows the shadow patterns of the discharge in nitrogen at pressure of 1 atm at various times. It can be seen that the discharge channel has a microstructure registered from the first nanoseconds after the breakdown. During this period the microchannel diameter is about 10 μm. By the twentieth nanosecond the discharge channel acquires a clear outer boundary, and then its radial expansion occurs. A similar pattern was also observed for the discharge in air [20].

Fig. 6 shows the shadow patterns of the discharge at various pressures in the range from 0.25 to 1 atm. All shadow patterns show a microchannel structure. At the

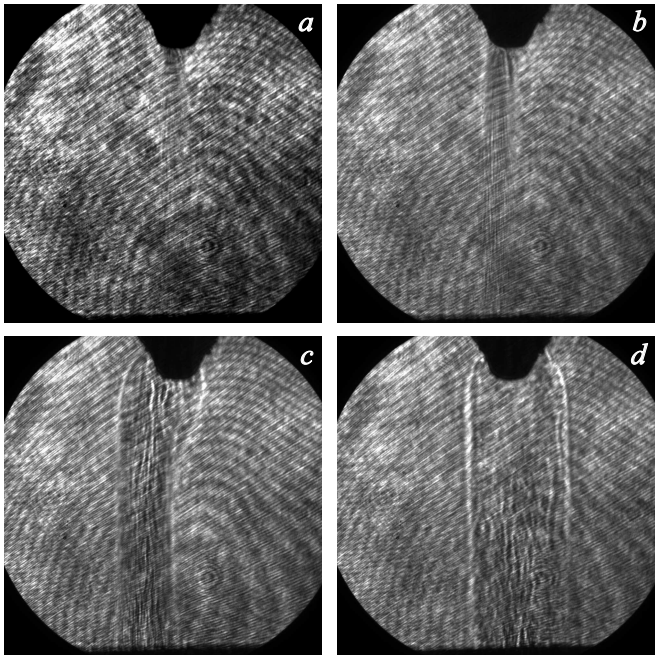

Figure 5. Shadow patterns of the glow of discharge in nitrogen at pressure of 1 atm at different times (*a* — 4, *b* — 7, *c* — 27, *d* — 60 ns).

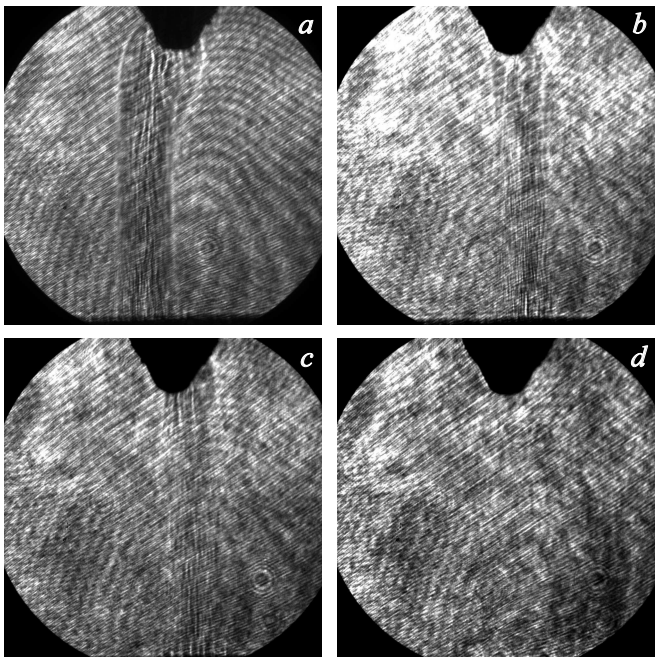

Figure 6. Shadow patterns of discharge in nitrogen at different pressures: *a* — 1 atm and 27 ns, *b* — 0.75 atm and 22 ns, *c* — 0.5 atm and 19 ns and *d* — 0.25 atm and 51 ns.

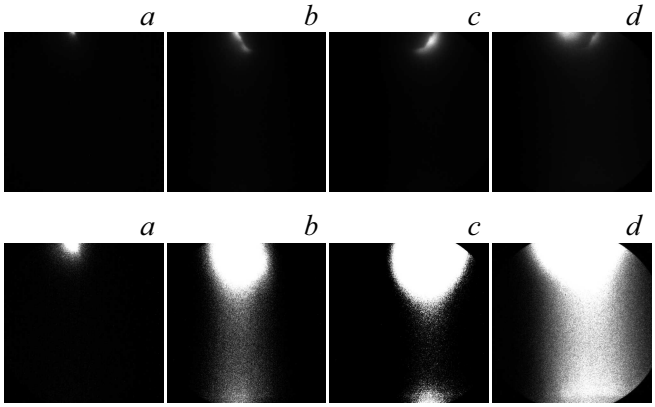

Figure 7. Photos of the glow of discharge in argon at pressure of 0.5 atm at different times: *a* — 10, *b* — 27, *c* — 52, *d* — 78.

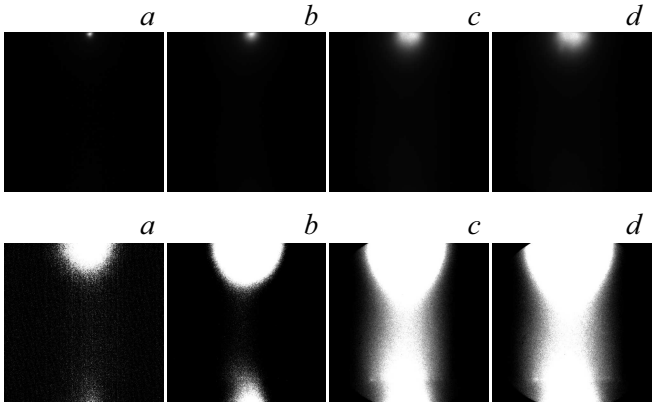

Figure 8. Photos of the glow of discharge in argon at pressure of 2 atm at different times: *a* — 1, *b* — 23, *c* — 68, *d* — 78.

same time, at a pressure of 0.25 atm, the microchannels are obscure. The reason for this may be the insufficient sensitivity of the shadow photography method used under conditions of decreased gas density and its gradients with pressure decreasing.

Figs. 7 and 8 show frames of the glow of the discharge in argon at pressure of 0.5 and 2 atm at different times. The images of the bottom row in each of Figs. 7 and 8 are computer-processed (with brightness increasing) images of the top row. This procedure makes it possible to visualize the structure of the glow of the discharge regions with a relatively low intensity. See that the glow in the initial stage of the discharge manifests itself in the form of cathode spots and a weak diffuse glow along the entire length of the gap, after which a relatively bright luminous anode region is formed. In this case, the main region of the discharge has a relatively low glow intensity. Just as for nitrogen, a similarity in the morphology of the luminescence structure at different pressures can be traced. However, it should be noted that unlike nitrogen and air [18,20] the discharge in argon has a diffusion nature. This is also evidenced by the shadow patterns of the discharge in argon (Fig. 9), in which the discharge region with a clearly defined boundary becomes clearly distinguishable only at later stages. Since the oscillograms give close values of the discharge current in air, nitrogen, and argon, we can conclude that its distribution in the discharge gap is more uniform in the latter case.

At all pressures used here, a microstructure is recorded on the shadow patterns of the discharge in argon (Fig. 9): the discharge in argon is a dense set of micron-diameter channels. For example, at the argon pressure of 2 atm at time 27 ns the microchannel diameter does not exceed 8 μm. In that, as in the case of nitrogen, the microstructure in argon becomes weaker with pressure decreasing, which can also be explained by the sensitivity decreasing of the shadow photography method. Also note that, as in the case of nitrogen and air, the microchannel structure is indistinguishable in the photographs of the glow of discharge in argon.

Thus, the presence of a discharge microstructure in nitrogen and argon both at high and low pressures should be indicated as the main result of the studies. Previously, the microstructure was discovered and studied in various types of discharges in air [11–25], which, unlike the gases used here, is electrically negative. The data obtained in this work, in particular, show that the electronegativity of the gas is not a necessary condition for the microstructure formation. Generally, the presented experimental data may indicate the widespread occurrence of the microstructuring phenomenon, which, apparently, is a result of the occurrence of universal regularities in the development of discharges.

The results obtained in this and some other papers make it necessary to take into account the microstructure presence in gas discharges. This is important both in the fundamental sense associated with the making of the corresponding

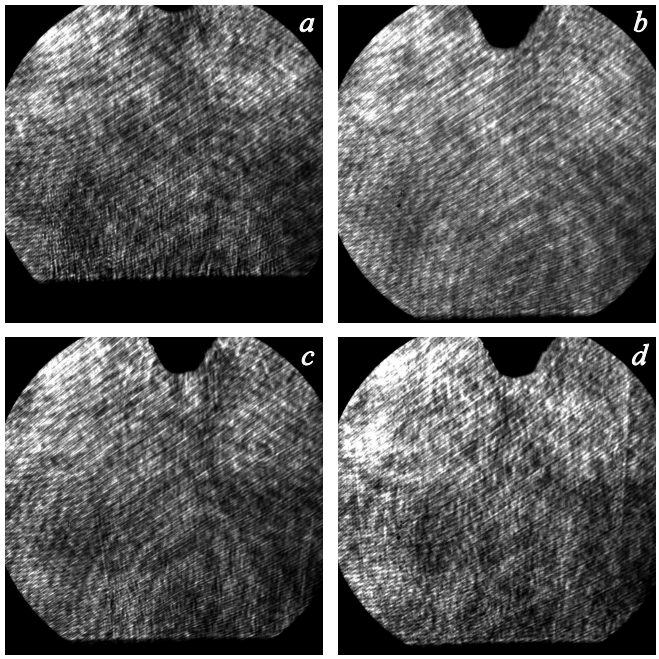

Figure 9. Shadow patterns of discharge in argon at different pressures: *a* — 2 atm and 92 ns; *b* — 1 atm and 49 ns; *c* — 0.8 atm and 99 ns; *d* — 0.5 atm and 169 ns.

computational and theoretical models of processes in gas discharges, and in the development and application of gas discharge technologies.

Conclusion

Using high-speed shooting and the shadow photography, the glow structure and the microstructure of a pulsed discharge in a 1.5 mm long gap „pin (cathode)−plane“ in nitrogen in the pressure range from 0.25 to 1 atm and in argon in the pressure range from 0.5 to 2 atm was studied.

It has been found that the spark discharge is realized in nitrogen. The dynamics of the glow structure includes successive phases: the appearance of cathode spots and a weakly luminous diffuse channel, the propagation of luminous formations from the cathode, and bridging the gap by a uniform, relatively thin, brightly luminous channel.

It is shown that the structure evolution of the glow of discharge in nitrogen delays relatively to the onset of breakdown with pressure decreasing; however, the morphology of the structure retains similarity at different pressures.

The presence of microstructure of the discharge in nitrogen in the studied pressure range was found — the discharge is a set of microchannels of micron-diameter from the first nanoseconds.

It was found that the dynamics of the glow structure and the microstructure of the discharge in nitrogen is similar to the discharge in air.

The dynamics of the glow of the discharge in argon, including the appearance of cathode spots and a weak diffuse glow along the entire length of the gap, and then the formation of the near-anode region of the glow, were registered. The discharge in argon has a diffuse nature with a relatively low glow intensity and a weakly expressed channel boundary, and the evolution of the discharge glow structure shows similarity at different pressures.

The presence of the microstructure of the discharge in argon in the studied pressure range was established — the discharge is a dense set of microchannels.

Conflict of interest

The authors declare that they have no conflict of interest.

References

[1] S.M. Starikovskaia. J. Phys. D: Appl. Phys., **47** (35), 353001 (2014). DOI: 10.1088/0022-3727/47/35/353001

[2] N.A. Popov. Plasma Sources Sci. Technol., **20** (4), 045002 (2011). DOI: 10.1088/0963-0252/20/4/045002

[3] N.L. Aleksandrov, S.V. Kindysheva, I.N. Kosarev, S.M. Starikovskaia, A.Y. Starikovskii. Proc. Combust. Inst., **32**, 205 (2009).

[4] Yang Liu, C. Kolbakir, A.Y. Starikovskiy, R. Miles, Hui Hu. Plasma Sources Sci. Technol., **28** (1), 014001 (2019). DOI: 10.1088/1361-6595/aaedf8

[5] A.Yu. Starikovskii, A.A. Nikipelov, M.M. Nudnova, D.V. Roupassov. Plasma Sources Sci. Technol., **18** (3), 034015 (2009). DOI: 10.1088/0963-0252/18/3/034015

[6] E. Moreau. J. Phys. D: Appl. Phys., **40** (3), 605 (2007). DOI: 10.1088/0022-3727/40/3/S01

[7] G.A. Mesyats, V.V. Osipov, V.F. Tarasenko. *Impulsnye gazovye lazery*(Nauka, M., 1991) (in Russian)

[8] A.I. Pavlovsky, V.F. Basmanov, V.S. Bosamykin, V.V. Gorokhov, V.I. Karelin, P.B. Repin. Kvant. elektron., **14** (2), 428 (1987) (in Russian)

[9] V.F. Tarasenko. *Impulsnye lazery na perekhodakh atomov i molekul*(SST, Tomsk, 2014) (in Russian)

[10] M. Erofeev, V. Ripenko, M. Shulepov, V. Tarasenko. Eur. Phys. J. D, **71**, 117 (2017). DOI: 10.1140/epjd/e2017-70636-6

[11] S.N. Buranov, V.V. Gorokhov, V.I. Karelin, A.I. Pavlovsky, P.B. Repin. Kvant. elektron., **18** (7), 891 (1991) (in Russian)

[12] A.V. Perminov, A.A. Trenkin. Tech. Phys., **50** (9), 1158 (2005).

[13] A.A. Trenkin, V.I. Karelin. Tech. Phys., **53** (3), 314 (2008). DOI: 10.1134/S1063784208030055

[14] P.B. Repin, A.G. Repiev. In sb.: *Issledovaniya po fizike gazovogo razryada,* pod red. V.D. Selemira and A.E. Dubinova (Sarov, 2003), p. 143 (in Russian)

[15] A.G. Rep'ev, P.B. Repin, V.S. Pokrovski'. Tech. Phys., **52** (1), 52 (2007).

[16] S.N. Buranov, V.V. Gorokhov, V.I. Karelin, P.B. Repin. ZhTF, **74** (10), 40 (2004) (in Russian)

[17] A.A. Tren'kin, V.I. Karelin, Yu.M. Shibitov, O.M. Blinova. Tech. Phys., **63** (10), 1473 (2018). DOI: 10.1134/S1063784218100237

[18] K.I. Almazova, A.N. Belonogov, D.V. Beloplotov, V.V. Borovkov, A.A. Tren'kin, M.V. Erofeev, V.S. Ripenko, M.A. Shulepov, V.F. Tarasenko. J. Nanosci., Nanomedic. Nanobiol., **4** (1), 1 (2021).

[19] A.A. Trenkin, K.I. Almazova, A.N. Belonogov, V.V. Borovkov, E.V. Gorelov, I.V. Morozov, S.Yu. Kharitonov. Tech. Phys., **63** (6), 801 (2018). DOI: 10.1134/S1063784218060026

[20] A.A. Trenkin, K.I. Almazova, A.N. Belonogov, V.V. Borovkov, E.V. Gorelov, I.V. Morozov, S.Yu. Kharitonov. Tech. Phys., **65** (12), 1948 (2020). DOI: 10.1134/S1063784220120270

[21] A.A. Trenkin, K.I. Almazova, A.N. Belonogov, V.V. Borovkov, E.V. Gorelov, I.V. Morozov, S.Yu. Kharitonov. Tech. Phys., **66** (2), 243 (2021). DOI: 10.1134/S1063784221020225

[22] E.V. Parkevich, M.A. Medvedev, A.I. Khirianova, G.V. Ivanenkov, A.S. Selyukov, A.V. Agafonov, K.V. Shpakov, A.V. Oginov. Plasma Sources Sci. Technol., **28**, 125007 (2019). DOI: 10.1088/1361-6595/ab518e

[23] E.V. Parkevich, M.A. Medvedev, G.V. Ivanenkov, A.I. Khirianova, A.S. Selyukov, A.V. Agafonov, Ph.A. Korneev, S.Y. Gus'kov, A.R. Mingaleev. Plasma Sources Sci. Technol., **28**, 095003 (2019). DOI: 10.1088/1361-6595/ab3768

[24] A.A. Tren'kin, K.I. Almazova, A.N. Belonogov, V.V. Borovkov, E.V. Gorelov, I.V. Morozov, S.Yu. Kharitonov. ZhTF, **92** (3), 348 (2022) (in Russian) DOI: 10.21883/JTF.2022.03.52130.235-21

[25] K.I. Almazova, A.N. Belonogov, V.V. Borovkov, V.S. Kurbanismailov, Z.R. Khalikova, P.Kh. Omarova, G.B. Ragimkhanov, D.V. Tereshonok, A.A. Trenkin. Phys. Plasmas, **27**, 123507 (2020). DOI: 10.1063/5.0026192

[26] V.I. Karelin, A.A. Trenkin, I.G. Fedoseev. Phys. Atom. Nucl., **78** (12), 1440 (2015). DOI: 10.1134/S1063778815120133

[27] A.A. Tren'kin, V.D. Beibalaev, G.B. Ragimkhanov. Nelineyny mir, **17** (5), 47 (2019) (in Russian)

[28] V.I. Karelin, A.A. Trenkin. High Voltage Engineer., **41** (2), 1 (2015).